Sborník vědeckých prací Vysoké školy báňské – Technické univerzity Ostrava
číslo 1, rok 2009, ročník LII, řada hutnická
článek č. 1439

EXPERIMENTAL OBSERVATION OF RUBBER BLENDS BY ATOM FORCE MICROSCOPE

D. BAKOŠOVÁ[1*], S. RUSNÁKOVÁ[1], I. LETKO[1], I. RUŽIAK[2]

[1*] *Faculty of Industrial Technologies in Púchov, University of Alexander Dubček in Trenčín, Department of Physical Engineering of Materials, Púchov, Slovak Republic, bakosova@fpt.tnuni.sk*
[2] *Faculty of Industrial Technologies in Púchov, Institute of material technological research, Púchov, Slovak Republic*

ABSTRACT: Application of SEM gives us very important information and it significantly supplements traditional materials analysis. This work deals with investigation of a surface by atomic force microscope (AFM). The work includes description and content of constituent rubber blends and description of constituent methods, which were used in measurement.

KEY WORDS: AFM, topography

1. INTRODUCTION

1.1 Atomic-force microscope

Atomic-force microscope (AFM NT - 206) in a complex with control and image processing software is intended for measurement and analysis of surface micro- and submicrorelief, objects of the micro- and nanometer range with high resolution [1].

Fields of application of the AFM are physics of solids, thin-film technologies, nanotechnologies; micro- and nanotribology, microelectronics, optics, testing systems of the precision mechanics, magnetic record, vacuum engineering etc.

The AFM can be used in scientific and industrial laboratories. The image of a surface in the AFM is obtained at scanning of a sample in a horizontal plane by a tip with the curvature radius about tens–hundreds of nanometers attached to the cantilever. Control system traces the probe position relative for the sample surface in every measurement point and adjusts the tip-to-sample separation at constant level set by the operator. The changes of the probe vertical position in every point make an AFM data matrix, which is recorded in a file and it can be later used for further processing, visualization and analysis [2].

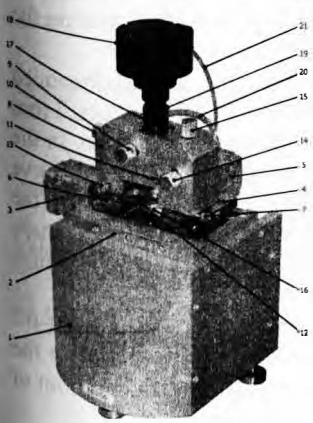

Fig. 1: Scanning unit of atomic force microscope NT-206. 1 – case (base platform); 2 – Y positioning stage; 3 – driving stepper motor of Y positioning stage; 4 – X positioning stage; 5 – driving stepper motor of X positioning stage; 6 – a dove tail couple for mounting the measuring head; 7 – screw for fixing the measuring head in dove tail; 8 – a measuring head; 9 – a knob of a laser source adjusting mechanism for X direction; 10 – a knob of a laser source adjusting mechanism for Y direction; 11 – a mirror axis; 12 – a probe holder; 13 – a screw for locking a probe holder; 14 – a knob of a photodetector adjusting mechanism for X direction; 15 – a knob of a photodetector adjusting mechanism for Y direction; 16 – sample platform on the piezoscanner top; 17 – a video system tube; 18 – a video camera module; 19 – a turnable ring for fine focusing of the video system; 20 – video system output cable (USB type); 21 – measuring head cable.

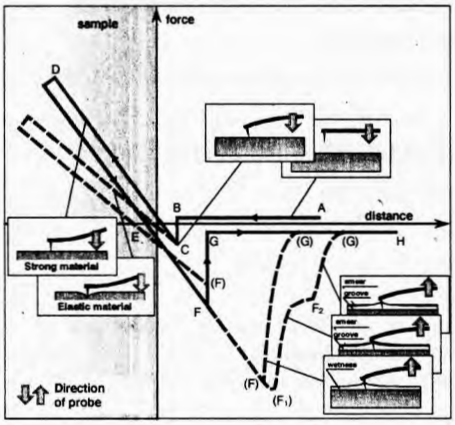

Fig. 2: Nomogram of the curves - approach/ moving off. Solid lines are schematic presentation of curves obtained in vacuum. Dashed lines show variations of curves of approach/moving off conditioned by elastic features of the sample and by presence of surface layers of moisture and streaks (impurities)

1.2 Possibility of atomic-force microscope

By using AFM it is possible to scan curves that show dependence of composite action force of the probe and surface of the sample on distance between them – these are the curves of approach /moving off. These curves are very important for measurements of vertical force attached to the surface from the side of the peak in the process of scanning. Besides the force, it is also possible to evaluate viscosity of dirty surface, thickness of the covering layer and also local variations of elastic features of the surface from the curve.

The curve of approach/moving off is a graphic dependence of measuring bracket deviation on scanning device extension. Van der Waals forces are only one factor of bracket deviation affecting. The measurement will also be influenced by thin layers of moisture that are usually present at working with AFM in the presence of air and also streaks and impurities. The curves of approach/moving off we obtain are specific enough for each sample and at the same time we can separate general characteristic sections in them, as shown in Fig. 2.

Section A-B. Scanning device is completely moved off in the left part and the bracket is not swaying because the peak is not touching the sample. By approaching the surface the bracket is not swaying until Van der Waals forces start to act (point B). In this part the curve does not contain any useful information.

Section B-C. In point B the bracket suddenly starts to move towards the surface and the peak touches the surface (point C). This part of the curve is known as "leap to contact". In the case of working in air environment, there will be a composite action of the surface moisture capillarity and also impurities, streaks and grease on the peak besides Van der Waals attractive forces and electrostatic forces. Change of the force in the part B-C of the curve can be related to the peak shrinkage in accordance to the Hook law ($F = -k\Delta x$). This allows us to evaluate the thickness of absorbed layer on the sample's surface.

Section C-D. This part characterizes further approach of the probe to the sample, it is accompanied by driving needle peak to the surface and by nearly linear curve of the bracket towards the surface. From the shape of the C-D section we can evaluate modulus of elasticity of the system probe – surface. In the case that, for example, the measuring probe is much softer than the surface of the sample, the curve inclination presents mostly elastic constant of the bracket itself. Contrariwise, if the hardness of the bracket is much harder than the surface of the sample, inclination of the section C-D allows us to study elastic features of the sample. Section C-D doesn't have to be straight line at all, the inclination change of this curve part shows differences in surface reactions to different attached force [3].

Section D-E. Point D refers to the end of the approaching phase and the beginning of moving-off from the surface. If there is no hysteresis of the scanning device, the section D-E is practically the same as the section of the curve C-D, which we obtained during the approach. In the case that both of

these sections are straight and parallel, they do not give us any additional information (besides above mentioned). In the case that they are unparallel it allows us to determine plastic and elastic deformation of the sample (if the speed of recovery of surface geometrical features is slower than moving-off of the probe).

Section E-F. Point E refers to the neutral divergence of the bracket. During further moving-off of the probe from the surface, the bracket starts to incline to the sample because adhesive or gravity force affects the peak. The form of the section E-F is influenced by presence of absorbing layers on the sample's surface. In the case of vacuum work, Van der Waals and electrostatic forces affect the peak of the needle. If we work in air, quite strong capillary force of surface layer of moisture, grease and impurities adds to these forces. Thickness of the surface layer, influences the length of the section E-F and its inclination, which is different than inclination caused by hardness of the sample, as well as points at rising of absorbing layers together with the moving-off probe. When the elastic response of the bracket outruns gravity forces of the surface side and its layers, the probe separates from the sample surface. Point F, known as the point of separation, refers to this action in the curve of approach/moving off.

Section F-G. When the elastic response of the bracket outruns the gravity force of the surface and its layers, the probe separates from the sample. In the curve of approach/moving-off there is a point F, known as the point of separation, referring to this. The size of a straining in the point F is equal to the total maximum adhesive force between the probe and sample and provides key information on observation of adhesion. If the moisture layer is covered enough with grease layer or other impurities, it is the case when we can observe more than one point of separation (F1 and F2). Position of the points F1 and F2 depends on viscosity and thickness of these layers. Transition between the sections E-F and F-G does not necessarily have to have steep ascent. In the case that the absorbing layer has equal viscosity, the probe can move off from the surface gradually and the transition E-F-F-G will have round shapes.

2. EXPERIMENTAL PART

The sample composition was as is described in Tab. 1.

Tab.1: Composition of the studied samples

Components	Dose in DSK
SULPHUR	2-3
SULFENAX	1-2
KRALEX	130-145
VULCAN	85-100
ZnO	4-9
DUSANTOX	1-2
FLECTOL	1.3-1.6
STEARIN	1.7-2.2

The samples were characterized by inhomogeneities, which we can demonstrate by scanning the spectroscopic curve displaying dependence of a force concurring sound and surface of sample.

We employed the general approximation and Snedonn's formula for analysis dates and calculation of Young's modulus off complete rake curve.

The Sneddon's model gives the relationship between load gradient, dP/dh, and Young's modulus, E, in the form [4-6]:

$$\frac{dP}{dh} = \frac{2A^{1/2}}{\pi^{1/2}} E \qquad (1)$$

Where $$E = \left\{ \left[\left(1 - \nu_1^2\right) / E_1 \right] + \left[\left(1 - \nu_2^2\right) \right] / E_2 \right\}^{-1} \quad (2)$$

is composite elastic modulus,

E_1, E_2, ν_1, ν_2 -Young's module and Poisson's ratio of a material and an indenter, respectively,

P - normal load,

A - contact area,

h - the indentation depth.

On the basic equation 1 and 2 we can consider for E_1 and E_2:

$$\frac{dP_1}{dh_1} = \frac{2A^{1/2}}{\pi^{1/2}} E_1 \Rightarrow E_1 = \frac{dP_1}{dh_1} \frac{\pi^{1/2}}{2A^{1/2}} \qquad \frac{dP_2}{dh_2} = \frac{2A^{1/2}}{\pi^{1/2}} E_2 \Rightarrow E_2 = \frac{dP_2}{dh_2} \frac{\pi^{1/2}}{2A^{1/2}}$$

The relation of modulus of elasticity:

$$\frac{E_1}{E_2} = \frac{\frac{dP_1}{dh_1} \frac{\pi^{1/2}}{2A^{1/2}}}{\frac{dP_2}{dh_2} \frac{\pi^{1/2}}{2A^{1/2}}} \Rightarrow \frac{E_1}{E_2} = \frac{\frac{dP_1}{dh_1}}{\frac{dP_2}{dh_2}} \qquad \text{where } \frac{dP_1}{dh_1} = k_1 \text{ and } \frac{dP_2}{dh_2} = k_2 \Rightarrow \frac{E_1}{E_2} = \frac{k_1}{k_2}$$

The linear equation is: $y = kx + q$, $k = \frac{dP}{dh}$

Graph 1

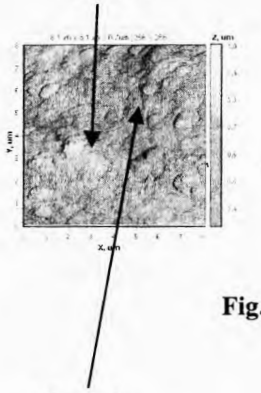

Graph 2

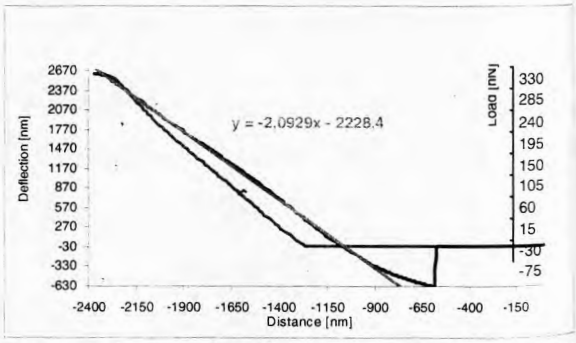

Fig. 3: Approximation of spectroscopic curve for calculation of Young's modulus

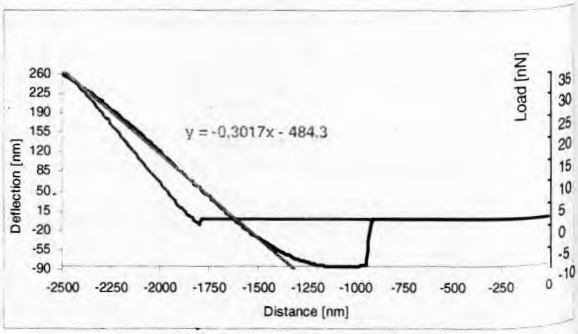

Fig. 4: Approximation of spectroscopic curve for calculation of Young's modulus

We obtained values of line by approximation curve to line from graph 1 and 2:

$k_1 = -2.0929$

$k_2 = -0.3017$

$$\Rightarrow E_1 = \frac{k_1 E_2}{k_2} = \frac{-2{,}0929}{-0{,}3017} E_2$$

$$E_1 = 6{,}937 E_2$$

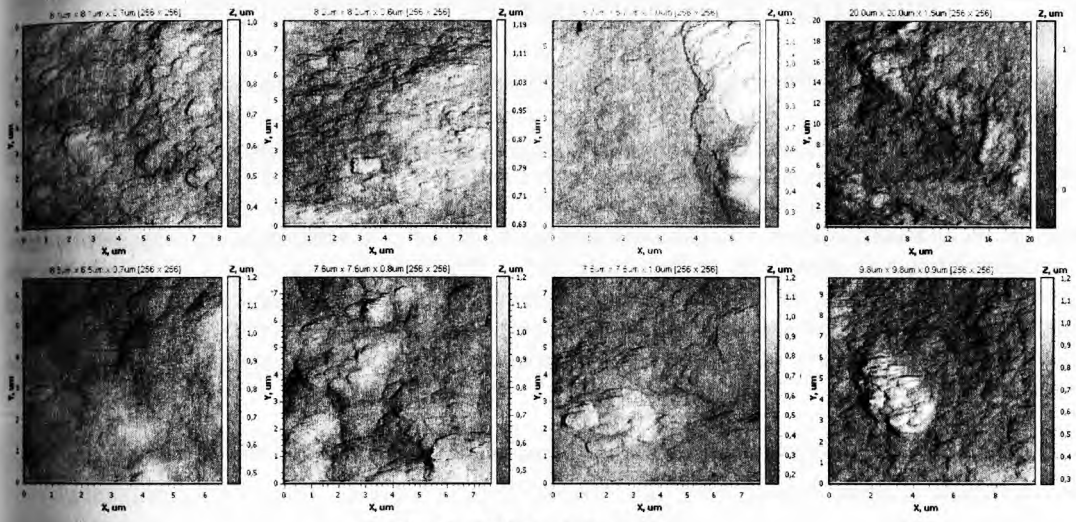

Fig. 5: AFM tested samples

4. RESULTS

We determined and calculated from the graphs, that Young's modulus of elasticity in measured point 1 is 6.937 multiple higher than in measured point 2. We can conclude that tested rubber mixture is not homogeneous.

5. REFERENCES

[1] WIESENDANGER, R.: *Probe Microscopy and Spectroscopy: Methods and Applications,* Cambridge University Press, 1994.

[2] Manual AFM NT, 206.

[3] HUTTER, J.L., BECHHOEFER, J.: Journal of Vacuum Science and Technology B, 12, 1994, 2251-2253.

[4] TSUKRUK, V.V., HUANG, Z., CHIZHIK, S.A., GORBUNOV V.V.: Journal of Materials Science, 33, 1998, 4905-4909.

[5] RATNER, B., TSUKRUK V.V.: *Scanning probe microscopy of polymers*, ACS Symposium Series, Washington DC, v. 694, 1997.

[6] BLIZNYUK, V.N., HAZEL, J., WU, H.J., TSUKRUK, V.V.: *Scanning probe Microscopy of polymers*, ACS Symposium Series, Washington DC, v. 690, 1997.